Journal of Surgical Radiology

Site: https://journalsurgrad.com/

ISSN Print 2156-213X| ISSN Online: 2156-4566 Volume: 05 Issue: 06 Open Access

Research Article

Ultrasound and Magnetic Resonance Imaging in Evaluating the Peripheral Nerves in Patients with Clinically Detected Leprosy Having Peripheral Neuropathy

Dr. M Vinod Kumar[1], Dr. T Arul Dasan[1], Dr. Sirish Shivaramaiah[2]

[1]Department of Radiodiagnosis, Bangalore Medical College and Research Institute (BMCRI), Bengaluru, Karnataka, India.

[2]Department of Radiology, Bangalore Medical College and Research Institute (BMCRI), Bengaluru, Karnataka, India.

*Corresponding Author
Dr. Sirish Shivaramaiah
Email: sirishs7@gmail.com.

Article History
Received: 10-05-2026
Revised: 23-05-2026
Accepted: 11-06-2026
Published: 24-06-2026

Citations:
Kumar MV, Dasan TA, Shivaramaiah S. Ultrasound and magnetic resonance imaging in evaluating the peripheral nerves in patients with clinically detected leprosy having peripheral neuropathy. J Surg Radiol, V5 (6) 587-601

Abstract: ***Introduction:*** Hansen's disease remains a leading treatable cause of peripheral neuropathy in endemic regions, with nerve damage often persisting despite bacteriological cure due to under-recognized peripheral neuritis. Clinical palpation and electrodiagnostic testing have limited sensitivity and reproducibility, whereas high-resolution ultrasonography (HRUS) and MRI/MR neurography enable direct visualization of nerve morphology, thickening, and inflammation. This study examines the spectrum of nerve alterations detected by HRUS and MRI in patients with clinically established leprosy and compares the diagnostic utility of the two modalities in assessing nerve involvement. **Objective:** To describe the spectrum of peripheral-nerve alterations demonstrated by high-resolution ultrasonography (HRUS) and magnetic resonance neurography (MRN) in patients with clinically detected leprosy neuropathy, and to compare the two modalities in detecting nerve involvement. **Methods:** In this hospital-based, prospective cross-sectional observational study, 40 consecutive patients with clinically or microbiologically diagnosed leprosy and clinical evidence of peripheral neuropathy underwent HRUS (high-frequency 10–18 MHz linear probes) and 1.5-Tesla MRN of the ulnar, median and posterior tibial nerves. Cross-sectional area (CSA), echotexture, fascicular architecture, endoneural Doppler flow, T1/T2/STIR and fat-suppressed signal, post-contrast enhancement and osteofibrous tunnel compression were assessed. Data were analysed with Student's t-test, the McNemar test, kappa statistics and receiver operating characteristic (ROC) analysis; a p-value ≤ 0.05 was considered significant. **Results:** The mean age was 39.42 ± 14.488 years with an equal sex distribution (50% female, 50% male). Lepromatous (45%) and borderline (35%) forms predominated. The ulnar and posterior tibial nerves were most frequently involved (35% each), followed by the median nerve (30%). Mean CSA was 20.58 ± 5.272 mm² for the ulnar, 19.73 ± 4.788 mm² for the posterior tibial and 17.18 ± 4.557 mm² for the median nerve. HRUS commonly demonstrated loss of fascicular architecture and heterogeneous echotexture, while MRN showed T2/STIR hyperintensity, nerve enlargement and post-contrast enhancement. HRUS and MRN detected nerve compression at comparable rates (McNemar p = 0.167–0.815) but agreement was only slight to poor ($\kappa = -0.133$ to 0.093). Posterior tibial CSA was significantly higher in patients without a history of reversal reaction (21.25 vs 18.2 mm²; p = 0.042). ROC analysis showed fair discrimination of CSA for MRI-detected compression (median AUC 0.701, p = 0.019; ulnar AUC 0.682, p = 0.042). Conclusion: HRUS is an effective, accessible screening tool for detecting structural nerve changes, whereas MRN provides additional information on neuritis and deep-nerve involvement. The two modalities are complementary rather than interchangeable, and their combined use improves diagnostic accuracy in leprosy-related neuropathy.

Keywords: Leprosy; Peripheral neuropathy; High-resolution ultrasonography; Magnetic resonance neurography; Nerve cross-sectional area.

INTRODUCTION

Hansen's disease remains one of the most important chronic infectious neuropathies worldwide and is among the most frequent treatable causes of peripheral neuropathy, particularly in developing countries where diagnostic delay contributes substantially to long-term disability [1]. The causative organism, *Mycobacterium leprae*, exhibits a strong tropism for Schwann cells and macrophages, producing segmental demyelination, axonal degeneration, neural fibrosis and progressive sensory and motor impairment when left untreated. Although global control programmes have markedly reduced disease prevalence, the infection remains endemic in many tropical and subtropical regions, and nerve damage may persist or progress even after bacteriological cure [2]. In India, national programme data show a decline in prevalence from 0.69 per 10,000 population in 2014–15 to 0.45 per 10,000 by 2021–22, with a fall in the annual new case detection rate from 9.73 to 5.52 per 100,000 population over the same period; despite this progress, a considerable proportion of patients still present with grade-1 and grade-2 disability, largely because of undetected or under-recognised peripheral neuropathy [3].

Neural involvement is central to the pathogenesis of Hansen's disease, and early identification of inflammatory neuritis is crucial because timely corticosteroid therapy and, where indicated, nerve

decompression can prevent or reverse permanent deformity. Traditionally, clinical examination and electrodiagnostic testing have been the mainstays of assessing nerve involvement. However, clinical palpation of thickened nerves is subjective, prone to inter-observer variability and often unreliable when nerves are deep-seated or when thickening is mild or segmental [4]. Electrodiagnostic studies detect functional deficits but have limited utility in delineating the anatomical extent of disease, are technically demanding, require specialised expertise and may fail to detect early inflammation or structural abnormality before functional impairment occurs [5].

In this context, imaging modalities such as high-resolution ultrasonography (HRUS) and magnetic resonance imaging (MRI), including MR neurography (MRN), have emerged as valuable non-invasive tools that allow direct visualisation of nerve morphology, fascicular architecture, epineurial thickness, signal characteristics, vascularity and the presence of intraneural oedema or compression [6]. HRUS provides real-time, high-resolution assessment of peripheral nerves and is particularly suited to the superficial nerves commonly affected in leprosy, such as the ulnar, median and posterior tibial nerves. It can detect focal or diffuse nerve enlargement, loss of the fascicular pattern, hypoechoic intraneural areas indicative of oedema or inflammation, epineurial thickening and increased endoneural vascularity on Doppler imaging—features that may be present even before functional impairment becomes clinically obvious [7]. HRUS is also cost-effective, widely accessible, repeatable and capable of surveying long nerve segments, making it particularly advantageous in resource-limited settings, and it can identify entrapment neuropathies that may coexist with or mimic leprosy neuropathy [8].

MRI and MRN provide complementary information through excellent contrast resolution and the ability to interrogate deep nerves, plexuses and proximal segments that are difficult to evaluate with ultrasound. MRI can depict nerve enlargement, fascicular disruption, T2-weighted hyperintensity representing inflammation or oedema, and post-contrast enhancement indicating breakdown of the blood–nerve barrier [9]. MRN can delineate the longitudinal extent of nerve involvement, identify skip lesions and differentiate active inflammation from chronic fibrosis, and is essential for detecting central or proximal lesions that, although uncommon, have been documented in advanced disease [10, 11]. Comparative studies of HRUS and MRI have shown concordance in detecting nerve pathology, with MRI offering superior evaluation of deeper structures and ultrasound providing greater spatial resolution for superficial nerves; nevertheless, their routine application in leprosy remains limited by lack of awareness, expertise and standardised imaging criteria [12].

The diagnostic challenge in leprosy lies in its variable presentation, ranging from mild sensory loss to severe polyneuropathy with disabling deformity. Nerve thickening, one of the most recognisable clinical features, is often subtle and may be missed early.

Reactions—particularly Type 1 (reversal) reactions—are associated with acute neuritis and require prompt recognition to prevent irreversible damage [13]. Imaging therefore has a pivotal role not only in diagnosis but also in disease monitoring: HRUS-measured cross-sectional area (CSA) provides an objective, reproducible parameter of severity and treatment response, while MRI helps differentiate active inflammation from chronic neuropathic damage [14]. However, systematic comparative research on the relative diagnostic utility of HRUS and MRI in the Indian population remains scarce, and previous studies have had small samples and heterogeneous protocols [15]. The present study was designed to systematically examine peripheral nerves using both HRUS and MRI in patients with clinically established leprosy presenting with peripheral neuropathy, with two objectives: first, to examine, assess and describe the spectrum of nerve alterations demonstrated by ultrasonography and MRI; and second, to compare the two modalities in detecting nerve involvement in leprosy.

MATERIALS AND METHODS

Study design and setting

This was a hospital-based, cross-sectional observational study with prospective consecutive enrolment, conducted in the Department of Radiodiagnosis at Bangalore Medical College and Research Institute (BMCRI), Bengaluru—a tertiary-level referral centre. The cross-sectional framework enabled simultaneous evaluation of the clinical, sonographic and MR neurographic characteristics of peripheral nerves at a single time point, without therapeutic intervention that might alter disease status, and was well suited to comparing the relative sensitivity of ultrasonography (USG) and MRI in detecting morphological abnormalities. Patients were referred from the outpatient and inpatient units of the Department of Dermatology, Venereology and Leprosy, where the diagnosis of Hansen's disease had been established on clinical evaluation and microbiological confirmation. The study was conducted from April 2024 to September 2025.

Participants

Patients were eligible if they were clinically or microbiologically diagnosed with leprosy; presented with symptoms or signs suggestive of peripheral neuropathy (nerve thickening, sensory loss, motor weakness or nerve tenderness); were willing to provide written informed consent (or assent for minors aged 12–18 years with parental consent); and were referred from

the Dermatology outpatient department or admitted to the wards of BMCRI.

Patients were excluded if they had leprosy without clinical evidence of peripheral neuropathy; had pre-existing neuropathies unrelated to leprosy (diabetes mellitus, alcoholism, traumatic nerve injury, hereditary neuropathies); had contraindications to MRI such as pacemakers, cochlear implants, metallic foreign bodies, claustrophobia or severe renal failure; declined to provide informed consent; or were unable to cooperate for imaging because of severe pain, limb deformity or acute medical conditions. These criteria ensured that the sample comprised individuals with clinically relevant nerve involvement while avoiding confounders that could mimic or obscure imaging findings. A consecutive sampling technique was used, and all eligible patients presenting during the study period who fulfilled the criteria and provided informed consent were recruited prospectively until the target sample size was reached.

Sample size

The sample size was determined using published CSA data from the study by Voltan et al., which evaluated ulnar nerve involvement in leprosy patients using ultrasonography [16]. Based on a standard deviation (σ) of ulnar-tunnel CSA of 3.2 mm², an absolute precision (d) of 1 mm², a Z value of 1.96 (95% confidence interval) and 80% power, the formula $n = Z^2\sigma^2/d^2$ yielded $n = (1.96^2 \times 3.2^2) = 39.3$. A final sample of 40 patients was therefore studied to ensure adequate statistical power.

Imaging technique / protocol

All patients underwent HRUS followed by MRN of the affected peripheral nerves. Ultrasonography was performed with high-frequency linear probes (10–18 MHz). Patients were positioned supine with the arm adducted for the median nerve, supine with the arm abducted for the ulnar nerve, and prone with the foot relaxed and hanging freely for the posterior tibial nerve. Each nerve was scanned longitudinally and transversely; the region of maximum enlargement or altered echotexture was identified, and CSA was measured using the direct trace method. Fascicular pattern loss, increased vascularity on colour Doppler, focal hypoechoic lesions and epineurial thickening were documented.

MRI was performed on 1.5-Tesla systems (Siemens Magnetom Avanto and uMR 570 wide-bore scanners) using dedicated surface or flexible coils, allowing multi-station evaluation of the peripheral nerves and plexuses. Sequences comprised axial and coronal T1-weighted imaging, axial and coronal T2/STIR imaging, fat-suppressed T2 sequences and post-contrast T1 imaging with fat suppression. For each nerve, the segment corresponding to the sonographic abnormality was targeted because the MRI coils provided a limited field of view. MRI assessed internal nerve signal characteristics, enhancement pattern, soft-tissue involvement, perineural oedema and tunnel stenosis. To limit inter-observer variability, all ultrasound examinations were performed by a single radiologist, and MRI studies were independently reviewed by two radiologists blinded to the ultrasound findings, with discrepancies resolved by consensus. Images were archived in PACS for review.

Statistical analysis

Data were entered into a structured database and analysed using SPSS software after verification and cleaning. Continuous data were summarised as mean ± standard deviation and categorical data as frequency and percentage. Student's t-test was used to compare CSA between groups; the chi-square test was used to test associations between qualitative imaging findings and clinical features; the McNemar test and Cohen's kappa (κ) were used to compare and assess agreement between USG and MRI in detecting nerve compression; and receiver operating characteristic (ROC) analysis was used to assess the diagnostic performance of CSA measurements. Sensitivity, specificity, and diagnostic indices were derived where appropriate. A p-value ≤ 0.05 was considered statistically significant. For subgroup analysis, patients were categorised by history of reversal reaction (present or absent), and nerve-wise analyses were performed for the ulnar, median and posterior tibial nerves. Reporting followed STROBE and STARD principles as applicable to an observational diagnostic study.

RESULTS

Demographic and clinical profile

Table 1. Demographic and diagnostic characteristics of the study population (n = 40).

Characteristic	Category	Frequency (n)	Percent (%)
Age (years)	Mean ± SD = 39.42 ± 14.488 (range 19–65)	—	—
Age group	<20	1	2.5
	20–30	13	32.5
	31–40	7	17.5
	41–50	6	15.0
	51–60	9	22.5
	>60	4	10.0

Gender	Female	20	50.0
	Male	20	50.0
Type of leprosy	Borderline	14	35.0
	Lepromatous	18	45.0
	Tuberculoid	8	20.0
Mode of diagnosis	Clinical	15	37.5
	Microbiological	25	62.5

Table 2. Pattern of nerve involvement, side distribution, clinical features and reversal-reaction history (n = 40).

Variable	**Category**	**Frequency (n)**	**Percent (%)**
Nerve involved	Median	12	30.0
	Posterior tibial	14	35.0
	Ulnar	14	35.0
Side	Bilateral	14	35.0
	Left	16	40.0
	Right	10	25.0
Motor weakness	No	19	47.5
	Yes	21	52.5
Nerve tenderness	No	17	42.5
	Yes	23	57.5
History of reversal reaction	No	20	50.0
	Yes	20	50.0

Table 3. Descriptive statistics of continuous clinical and imaging variables (n = 40).

Variable	N	Mean	SD	Minimum	Maximum
Duration of disease (months)	40	29.45	14.855	4	59
Ulnar CSA (mm²)	40	20.58	5.272	12	30
Median CSA (mm²)	40	17.18	4.557	10	25
Posterior tibial CSA (mm²)	40	19.73	4.788	11	28

Forty patients were studied. The mean age was 39.42 ± 14.488 years (range 19–65), with the majority in the young and middle-aged adult groups; 32.5% were aged 20–30 years and 22.5% were aged 51–60 years (Table 1). There was an equal sex distribution, with 20 women (50%) and 20 men (50%). Lepromatous leprosy was the most common type (45%), followed by borderline (35%) and tuberculoid (20%) forms. Diagnosis was microbiological in 25 patients (62.5%) and clinical in 15 (37.5%). The mean duration of disease was 29.45 ± 14.855 months (range 4–59) (Table 3).

The ulnar and posterior tibial nerves were each involved in 14 patients (35%), and the median nerve in 12 (30%). Involvement was left-sided in 40%, bilateral in 35% and right-sided in 25% (Table 2). Motor weakness was present in 21 patients (52.5%) and nerve tenderness in 23 (57.5%), indicating active neuritic involvement in more than half of the cohort. A history of reversal reaction was present in 20 patients (50%) (Table 2).

Continuous imaging variables

The mean cross-sectional area was greatest for the ulnar nerve (20.58 ± 5.272 mm²; range 12–30), followed by the posterior tibial nerve (19.73 ± 4.788 mm²; range 11–28) and the median nerve (17.18 ± 4.557 mm²; range 10–25) (Table 3; Figure 9).

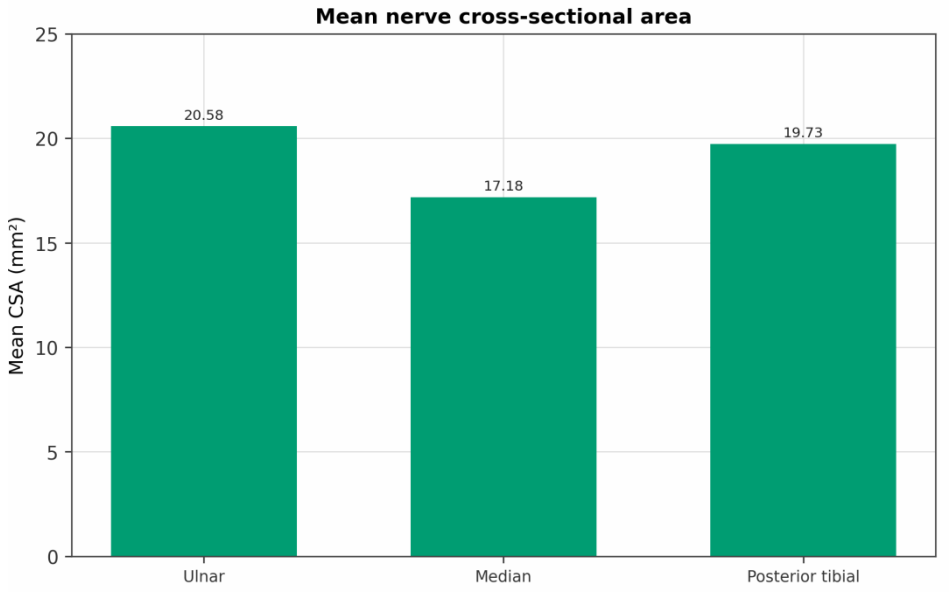

Figure 1. Mean cross-sectional area (CSA) of the ulnar, median and posterior tibial nerves on high-resolution ultrasonography; the ulnar nerve had the largest mean CSA (20.58 mm²) and the median nerve the smallest (17.18 mm²) (data from Table 3).

Ultrasonographic findings

Table 4. Ultrasonographic characteristics of the ulnar, median and posterior tibial nerves (n = 40).

Nerve	Parameter	Category	Frequency (n)	Percent (%)
Ulnar	Tunnel compression (USG)	No	21	52.5
		Yes	19	47.5
	Echotexture	Heterogeneous	23	57.5
		Hypoechoic	17	42.5
	Fascicular architecture	Lost	19	47.5
		Preserved	21	52.5
	Endoneural Doppler flow	Absent	22	55.0
		Present	18	45.0
Median	Tunnel compression (USG)	No	25	62.5
		Yes	15	37.5
	Fascicular architecture	Lost	24	60.0
		Preserved	16	40.0
	Echotexture	Heterogeneous	22	55.0
		Hypoechoic	18	45.0
	Endoneural Doppler flow	Absent	21	52.5
		Present	19	47.5
Posterior tibial	Tunnel compression (USG)	No	26	65.0
		Yes	14	35.0
	Fascicular architecture	Lost	24	60.0
		Preserved	16	40.0
	Echotexture	Heterogeneous	21	52.5
		Hypoechoic	19	47.5
	Endoneural Doppler flow	Absent	18	45.0
		Present	22	55.0

On HRUS, ulnar-tunnel compression was detected in 47.5% of patients, with heterogeneous echotexture in 57.5%, loss of fascicular architecture in 47.5%, and absent endoneural Doppler flow in 55% (Table 4; Figure 11); enlargement of the ulnar nerve with a hypoechoic fascicular pattern and increased cross-sectional area was a characteristic finding (Figure 1). For the median nerve, tunnel compression was seen in 37.5%, loss of fascicular architecture in 60%, heterogeneous echotexture in 55% and absent Doppler flow in 52.5%, with fusiform nerve enlargement on transverse imaging (Figure 2). For the posterior tibial nerve, tunnel compression was seen in 35%, loss of fascicular architecture in 60%, heterogeneous

echotexture in 52.5%, and present endoneural Doppler flow in 55% (Table 4); an increased cross-sectional area with loss of the normal fascicular definition was seen at the ankle (Figure 3).

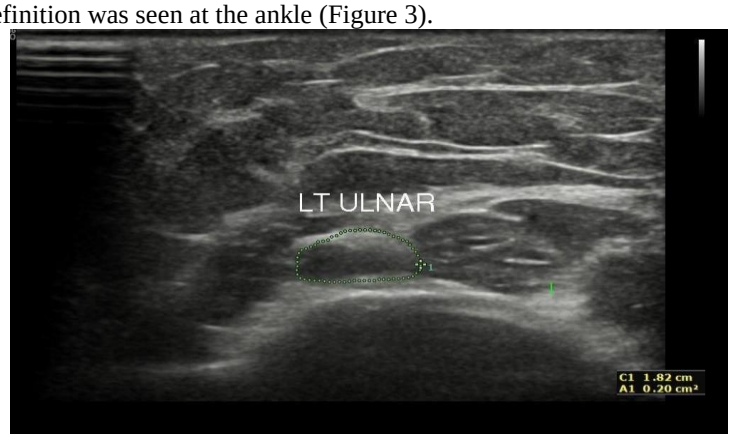

Figure 2. High-resolution ultrasonography of the left ulnar nerve at the elbow in a representative 60-year-old woman with Hansen's disease and peripheral neuropathy, showing diffuse nerve enlargement with a hypoechoic fascicular pattern and an increased cross-sectional area (direct-trace area 0.20 cm²), consistent with leprous neuritis.

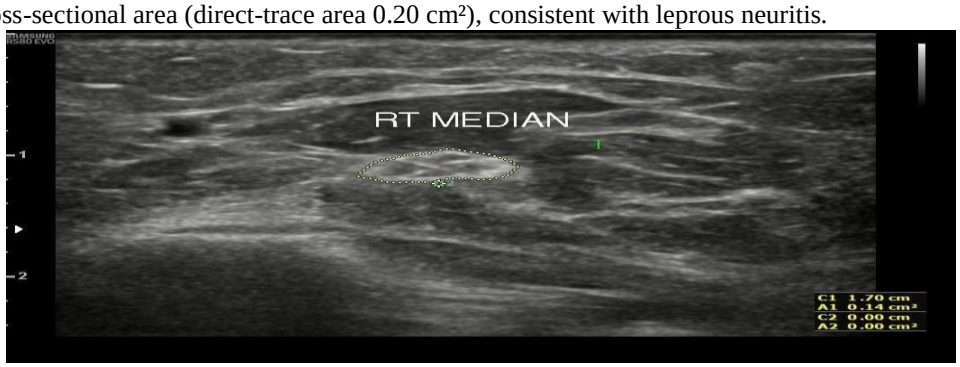

Figure 3. High-frequency ultrasound image of the right median nerve demonstrating mild fusiform enlargement with an increased cross-sectional area (direct-trace area 0.14 cm²), indicating peripheral nerve involvement.

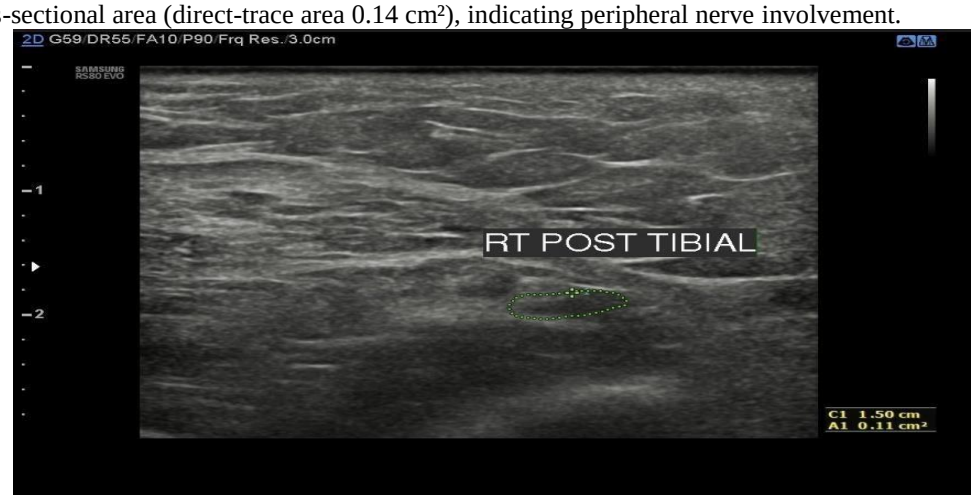

Figure 4. Ultrasonography of the right posterior tibial nerve at the ankle showing an increased cross-sectional area (direct-trace area 0.11 cm²) with loss of the normal fascicular definition, suggestive of leprous neuropathy.

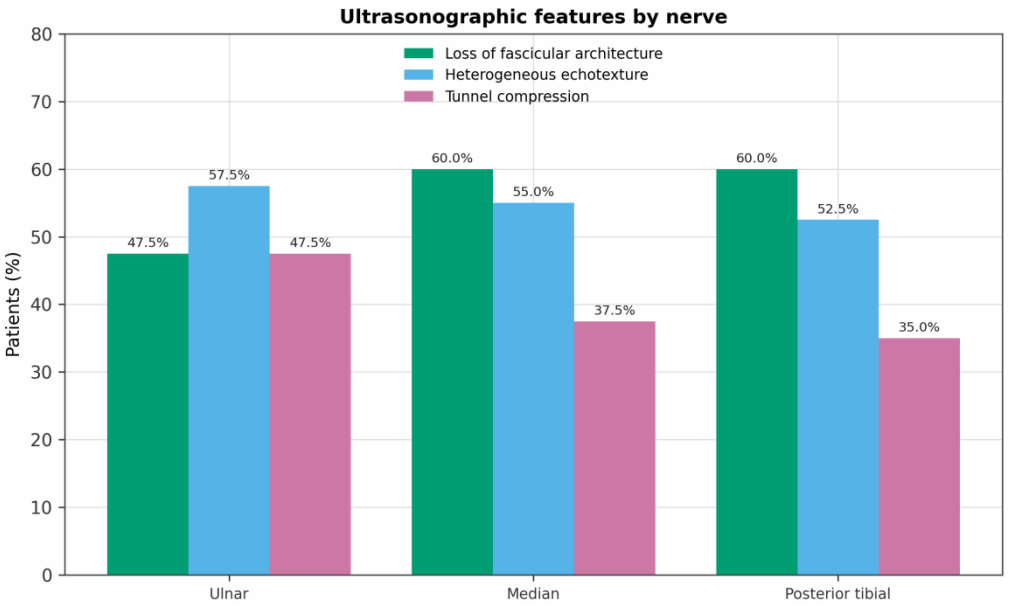

Figure5. Frequency of the principal ultrasonographic abnormalities—loss of fascicular architecture, heterogeneous echotexture and osteofibrous-tunnel compression—across the ulnar, median and posterior tibial nerves; loss of fascicular architecture was the most prevalent feature in each nerve (data from Table 4).

Table 5. MRI signal characteristics of the ulnar nerve (n = 40).

MRI parameter	Category	Frequency (n)	Percent (%)
T1 signal	Altered	20	50.0
	Normal	20	50.0
T2 signal	Hyperintense	25	62.5
	Normal	15	37.5
T2 FS signal	Hyperintense	16	40.0
	Mildly hyperintense	12	30.0
	Normal	12	30.0
STIR signal	Hyperintense	19	47.5
	Markedly hyperintense	6	15.0
	Mildly hyperintense	2	5.0
	Normal	13	32.5
Compression (MRI)	No	23	57.5
	Yes	17	42.5
Post-contrast enhancement	Increased	19	47.5
	Normal	21	52.5

Table 6. MRI characteristics of the median nerve (n = 40).

MRI parameter	Category	Frequency (n)	Percent (%)
T1 signal	Altered	24	60.0
	Normal	16	40.0
T2 signal	Hyperintense	18	45.0
	Normal	22	55.0
T2 FS signal	Hyperintense	14	35.0
	Mildly hyperintense	7	17.5
	Normal	19	47.5
STIR signal	Hyperintense	12	30.0
	Markedly hyperintense	6	15.0
	Mildly hyperintense	4	10.0
	Normal	18	45.0
Enlargement (MRI)	No	13	32.5
	Yes	27	67.5
Compression (MRI)	No	18	45.0
	Yes	22	55.0

Post-contrast enhancement	Increased	21	52.5
	Normal	19	47.5

Table 7. MRI characteristics of the posterior tibial nerve (n = 40).

MRI parameter	Category	Frequency (n)	Percent (%)
T1 signal	Altered	16	40.0
	Normal	24	60.0
T2 signal	Hyperintense	16	40.0
	Normal	24	60.0
T2 FS signal	Hyperintense	4	10.0
	Markedly hyperintense	7	17.5
	Mildly hyperintense	9	22.5
	Normal	20	50.0
STIR signal	Hyperintense	12	30.0
	Markedly hyperintense	4	10.0
	Mildly hyperintense	4	10.0
	Normal	20	50.0
Enlargement (MRI)	No	19	47.5
	Yes	21	52.5
Compression (MRI)	No	19	47.5
	Yes	21	52.5
Post-contrast enhancement	Increased	23	57.5
	Normal	17	42.5

MR neurographic findings

MRN of the ulnar nerve showed altered T1 signal in 50%, T2 hyperintensity in 62.5%, STIR hyperintensity (including markedly and mildly hyperintense) in 67.5%, MRI-detected compression in 42.5% and increased post-contrast enhancement in 47.5% (Table 5); across sequences the cubital-tunnel segment of the ulnar nerve showed fusiform enlargement, intraneural T2/STIR hyperintensity and loss of the normal fascicular pattern (Figures 4–7). For the median nerve, altered T1 signal was seen in 60%, T2 hyperintensity in 45%, nerve enlargement in 67.5%, MRI-detected compression in 55% and increased enhancement in 52.5% (Table 6), with diffuse thickening and increased signal of the nerve within the carpal tunnel (Figure 8). For the posterior tibial nerve, altered T1 signal was present in 40%, T2 hyperintensity in 40%, nerve enlargement in 52.5%, MRI-detected compression in 52.5% and increased enhancement in 57.5% (Table 7). MR neurography additionally depicted deep nerve segments and the lumbosacral plexus that lie beyond the reach of ultrasound.

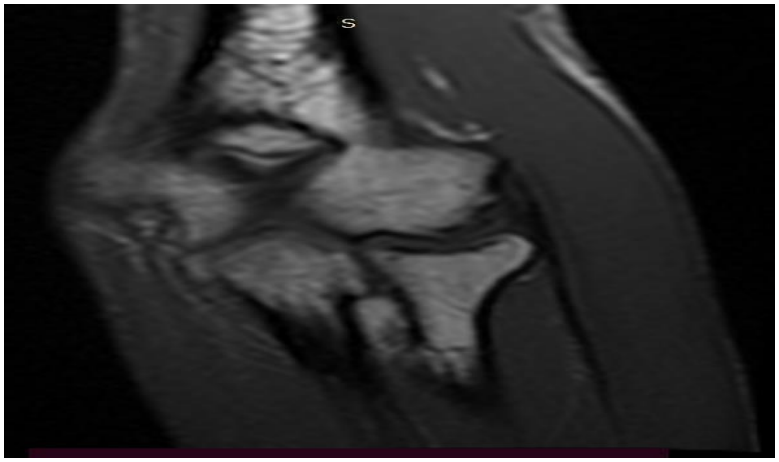

Figure 6. Coronal T1-weighted MR image of the right elbow showing mild fusiform enlargement of the ulnar nerve with relative effacement of the surrounding fat planes and no focal discontinuity.

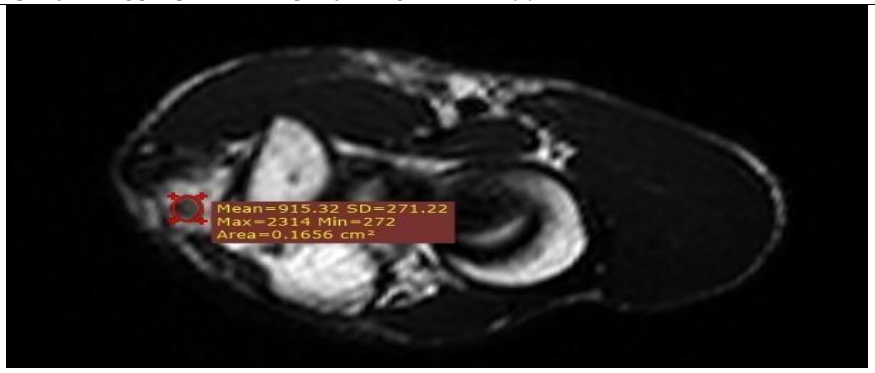

Figure 7. Axial T2-weighted MR image at the level of the right elbow demonstrating diffuse thickening of the ulnar nerve with mildly increased intraneural signal intensity and relative loss of the normal fascicular pattern (region-of-interest area 0.17 cm²).

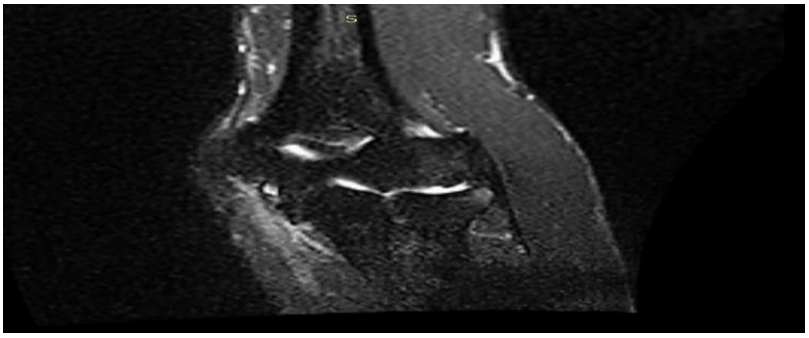

Figure 7. Coronal T2 fat-suppressed MR image of the right elbow demonstrating mild hyperintense signal and diffuse thickening along the course of the ulnar nerve in the cubital-tunnel region, consistent with inflammatory neuritis.

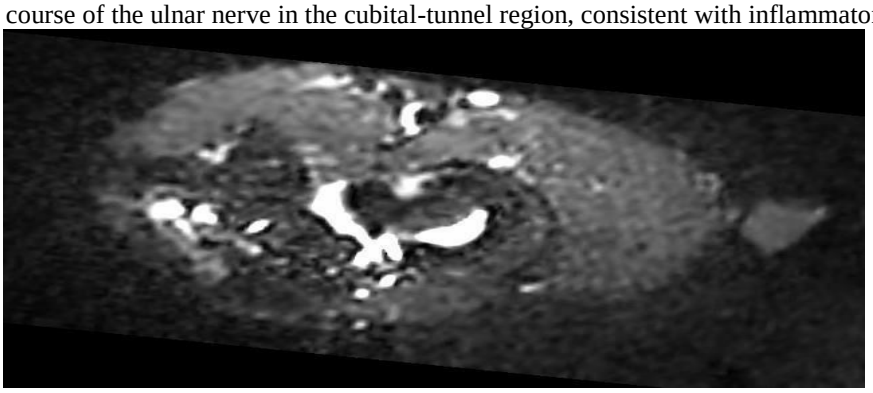

Figure 7. Axial STIR image at the level of the elbow showing a hyperintense, thickened ulnar nerve, suggestive of inflammatory neuritis.

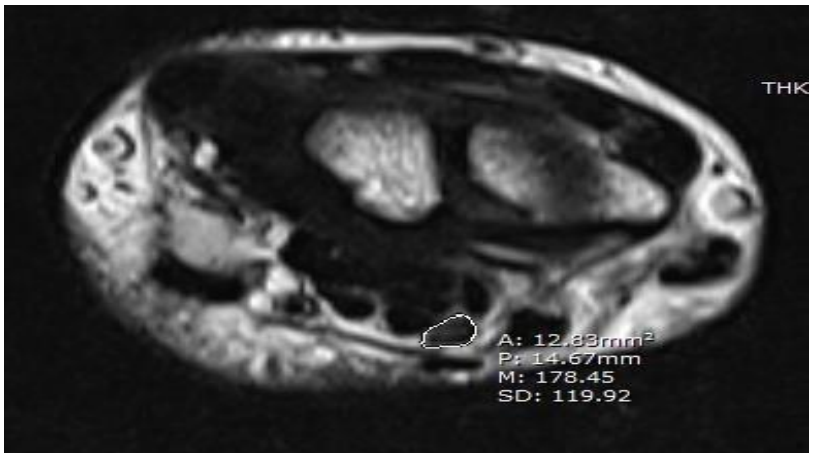

Figure 8. Axial T2-weighted MR image of the right wrist at the level of the carpal tunnel demonstrating mild diffuse thickening of the median nerve with increased signal intensity, loss of normal fascicular definition and an increased cross-sectional area (12.8 mm²), suggestive of inflammatory neuropathy.

Comparison of USG and MRI for nerve compression

Table 8. Comparison of nerve compression detected by USG and MRI, with McNemar test and kappa agreement (n = 40).

Nerve (USG compression)	MRI No	MRI Yes	Total	McNemar p	Kappa (κ)	Kappa p
Median — USG No	12	13	25	0.167	0.073	0.622
Median — USG Yes	6	9	15			
Median — Total	18	22	40			
Ulnar — USG No	13	8	21	0.815	0.093	0.554
Ulnar — USG Yes	10	9	19			
Ulnar — Total	23	17	40			
Posterior tibial — USG No	11	15	26	0.210	−0.133	0.370
Posterior tibial — USG Yes	8	6	14			
Posterior tibial — Total	19	21	40			

Table 9. Comparison of nerve cross-sectional area according to history of reversal reaction (n = 40).

Variable	History of reversal reaction	N	Mean	SD	t value	p value
Ulnar CSA (mm²)	No	20	20.8	5.644	0.267	0.791
	Yes	20	20.35	5.008		
Posterior tibial CSA (mm²)	No	20	21.25	4.711	2.101	0.042
	Yes	20	18.2	4.467		
Median CSA (mm²)	No	20	17.5	4.371	0.446	0.658
	Yes	20	16.85	4.826		

Table 10. ROC analysis of nerve cross-sectional area for prediction of MRI-detected nerve compression.

Test variable	State variable	AUC	95% CI	p value	Cut-off (mm²)	Sensitivity (%)	Specificity (%)
Ulnar CSA	MRI ulnar compression	0.682	0.515–0.848	0.042	17.5	82.4	68.2
Median CSA	MRI median compression	0.701	0.536–0.866	0.019	14.5	75.0	62.5
Posterior tibial CSA	MRI posterior tibial compression	0.644	0.472–0.816	0.101	18.5	81.0	55.6

The McNemar test showed no statistically significant difference between HRUS and MRN in detecting nerve compression for any of the three nerves: median (p = 0.167), ulnar (p = 0.815) and posterior tibial (p = 0.210), indicating comparable detection rates (Figure 10). However, agreement between the two modalities was low, with only slight agreement for the median (κ = 0.073; p = 0.622) and ulnar (κ = 0.093; p = 0.554) nerves and poor (negative) agreement for the posterior tibial nerve (κ = −0.133; p = 0.370) (Table 8; Figure 12).

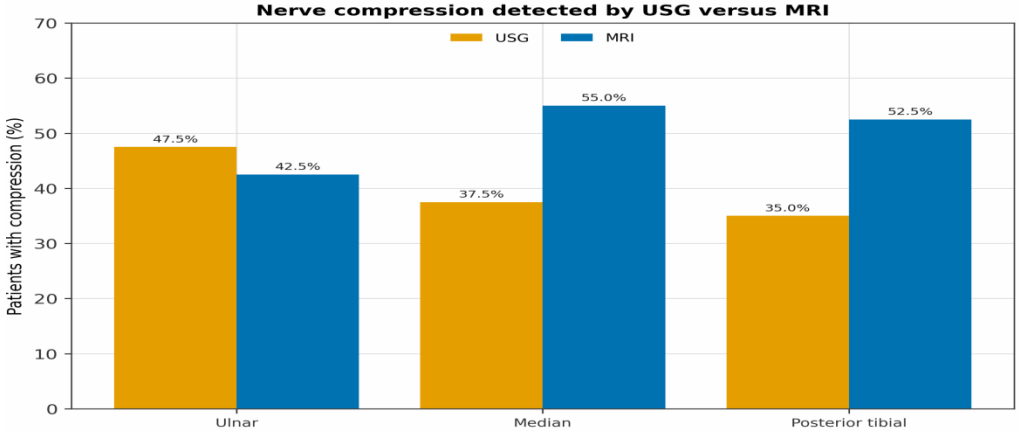

Figure 9. Proportion of patients in whom nerve compression was detected by high-resolution ultrasonography (USG) versus MRI for each nerve. The two modalities detected compression at comparable rates (McNemar p = 0.167–0.815) (data from Tables 4–7).

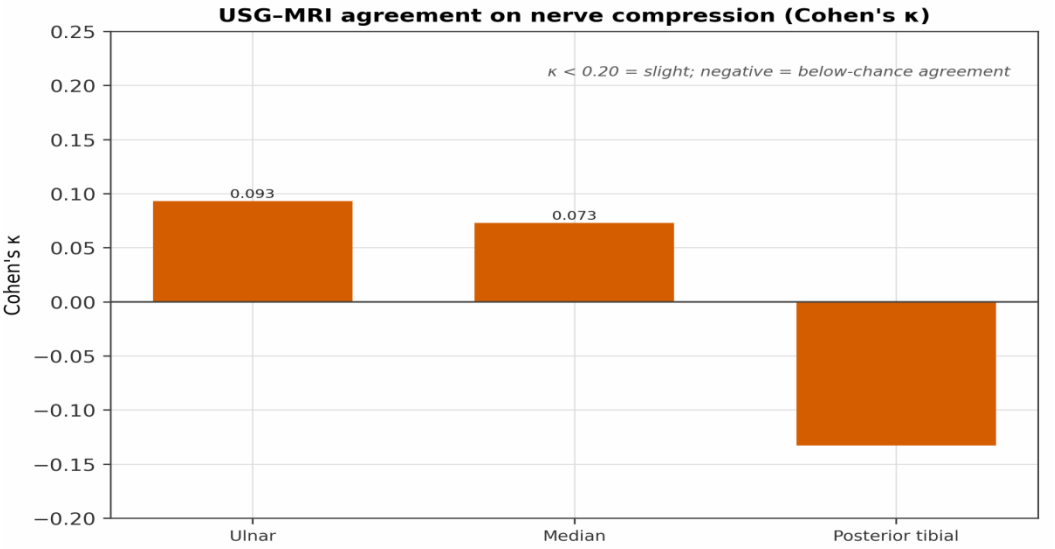

Figure 10. Inter-modality agreement (Cohen's κ) between USG and MRI for detecting nerve compression. Agreement was only slight for the ulnar (κ = 0.093) and median (κ = 0.073) nerves and below chance for the posterior tibial nerve (κ = −0.133), indicating that the two modalities are complementary rather than interchangeable (data from Table 8).

CSA and history of reversal reaction

Among the three nerves, only posterior tibial CSA showed a significant association with history of reversal reaction, being higher in patients without a reversal reaction (21.25 ± 4.711 mm²) than in those with one (18.2 ± 4.467 mm²; t = 2.101, p = 0.042). Ulnar CSA (20.8 vs 20.35 mm²; p = 0.791) and median CSA (17.5 vs 16.85 mm²; p = 0.658) did not differ significantly between groups (Table 9).

ROC analysis

ROC analysis of nerve CSA for predicting MRI-detected compression showed fair discriminatory ability for the median nerve (AUC 0.701; 95% CI 0.536–0.866; p = 0.019; cut-off 14.5 mm²; sensitivity 75.0%, specificity 62.5%) and the ulnar nerve (AUC 0.682; 95% CI 0.515–0.848; p = 0.042; cut-off 17.5 mm²; sensitivity 82.4%, specificity 68.2%), both statistically significant. Posterior tibial CSA showed modest, non-significant discrimination (AUC 0.644; 95% CI 0.472–0.816; p = 0.101; cut-off 18.5 mm²; sensitivity 81.0%, specificity 55.6%) (Table 10). The corresponding ROC curves are shown in Figures 11–13.

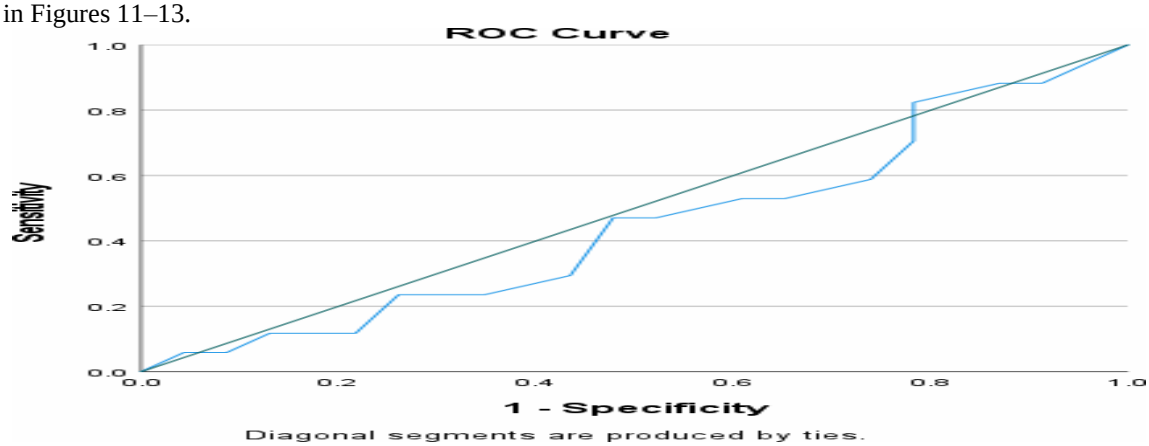

Figure 11. Receiver operating characteristic (ROC) curve of ulnar-nerve cross-sectional area for predicting MRI-detected ulnar compression, from the study's own ROC analysis (AUC 0.682; 95% CI 0.515–0.848; p = 0.042).

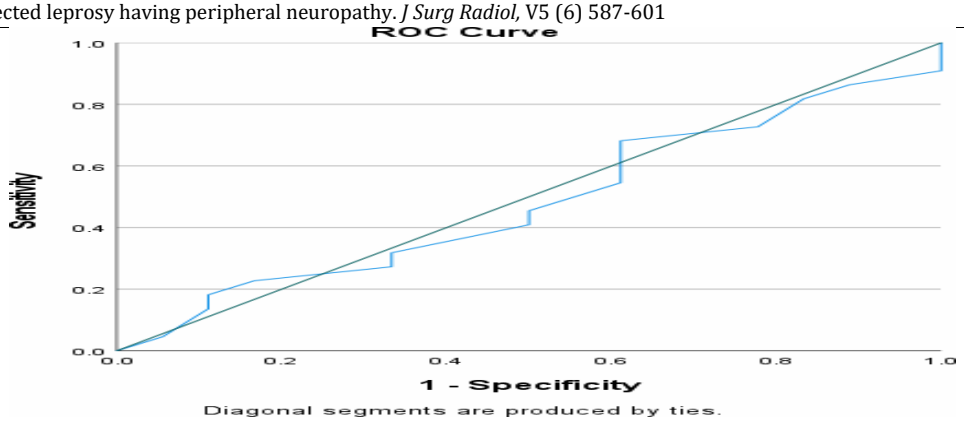

Figure 12. ROC curve of median-nerve cross-sectional area for predicting MRI-detected median compression, from the study's own ROC analysis (AUC 0.701; 95% CI 0.536–0.866; p = 0.019).

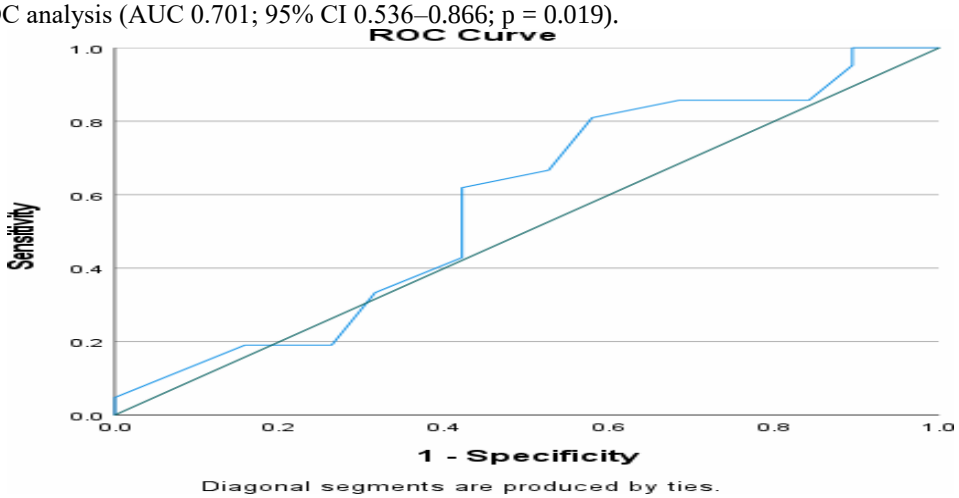

Figure 15. ROC curve of posterior tibial-nerve cross-sectional area for predicting MRI-detected posterior tibial compression, from the study's own ROC analysis (AUC 0.644; 95% CI 0.472–0.816; p = 0.101).

DISCUSSION

Peripheral neuropathy is the most significant cause of morbidity in Hansen's disease, frequently causing sensory loss, motor deficit and permanent disability if not detected early [15]. The present study evaluated the role of HRUS and MRN in clinically detected leprosy neuropathy and confirmed that both modalities capture the structural and inflammatory signatures of nerve involvement, while providing largely complementary information.

The mean age of approximately 39 years, with most patients in the young and middle-aged adult group, indicates that neuropathic manifestations of leprosy commonly affect the economically productive population, in whom disability carries a disproportionate socioeconomic cost [15]. The equal sex distribution may reflect changing epidemiological patterns, improved healthcare access and increased disease awareness among both sexes. Multibacillary (lepromatous and borderline) forms predominated, supporting the established association between higher bacillary load and greater neural involvement. The predominant affection of the ulnar and posterior tibial nerves, followed by the median nerve, is consistent with the known predilection of *M. leprae* for superficial nerves at anatomical entrapment sites and in relatively cooler regions of the body, and mirrors the distribution reported in multisegmental ultrasound and clinical series [13, 30]. That more than half of patients demonstrated motor weakness and nerve tenderness underscores the frequency of active neuritic involvement and the need for imaging that can detect structural change before irreversible functional deficit.

HRUS revealed characteristic increases in cross-sectional area, altered echotexture and loss of the normal fascicular architecture, reflecting inflammatory oedema, neural fibrosis and structural distortion, and enabled dynamic evaluation of compression at anatomical tunnel sites. These observations reinforce the value of ultrasonography as a readily available, cost-effective screening modality in endemic regions, in keeping with longitudinal and treatment-monitoring studies that have used sonographic parameters to track disease activity [26, 27]. Prior work has similarly shown that ultrasonography can detect subclinical nerve involvement earlier than clinical or electrophysiological assessment, and that qualitative features such as loss of fascicular definition and hypervascularity may precede measurable enlargement [17, 18]. Sonographic and multimodal case studies of focal ulnar and radial nerve swellings have further highlighted the diagnostic utility

of imaging in distinguishing leprosy neuropathy from compressive or neoplastic lesions [19, 22, 23].

MRN demonstrated T2/STIR hyperintensity, nerve enlargement and post-contrast enhancement—findings indicative of neuritis and inflammatory neuropathy—and provided superior visualisation of deep nerve segments and surrounding soft-tissue change. These patterns are concordant with reviews and technical studies of peripheral nerve MRI, which emphasise increased T2 signal, fascicular disorganisation and blood–nerve barrier breakdown as hallmarks of active disease, and with advanced techniques such as diffusion tensor imaging that quantify microstructural injury in leprous nerves [20, 21, 29]. MRI additionally offers the ability to detect proximal, plexus and rare central lesions that lie beyond the reach of ultrasound, extending the neuroimaging spectrum of Hansen's disease [11, 22].

Statistical comparison of nerve compression detected by HRUS and MRN using the McNemar test showed no significant difference for any nerve, indicating that both modalities identify comparable proportions of compression. However, kappa statistics revealed only slight—and, for the posterior tibial nerve, poor—agreement, suggesting that each modality detects compression in different subsets of patients. This supports the concept that HRUS and MRN are complementary rather than interchangeable, echoing integrated imaging strategies advocated for peripheral neuropathies in which ultrasound characterises superficial nerves and MRI captures deeper or proximal pathology [23, 24, 25]. The significant association of posterior tibial CSA with history of reversal reaction—higher CSA in patients without a reversal reaction—may reflect the dynamic and fluctuating nature of inflammatory swelling across reactional states, and warrants confirmation in longitudinal studies, whereas median and ulnar CSA showed no such association.

ROC analysis showed fair discriminatory performance of CSA for predicting MRI-detected compression, particularly for the median and ulnar nerves, whereas posterior tibial CSA had lower, non-significant predictive accuracy. These findings suggest that CSA is a useful screening parameter that should be interpreted alongside clinical and advanced imaging findings rather than in isolation, consistent with case-control and correlation studies of sonographic nerve measurements in Hansen's disease [25, 28]. Point-of-care ultrasound has been shown to reliably detect nerve thickening with strong concordance to high-resolution examination, supporting the feasibility of scaling ultrasound-based nerve assessment in field settings [16]. Overall, the study highlights the complementary diagnostic roles of the two modalities: ultrasonography provides rapid, dynamic and inexpensive assessment, while MRN offers superior soft-tissue characterisation and evaluation of deeper neural segments.

STRENGTHS AND LIMITATIONS

The strengths of this study include the systematic, protocol-driven evaluation of the same patients by both HRUS and 1.5-Tesla MRN, the use of a single operator for ultrasonography and two blinded readers for MRI to reduce inter-observer variability, and the objective quantification of nerve CSA with formal statistical comparison including McNemar, kappa and ROC analyses.

The study also has several limitations. First, the sample size was relatively small (n = 40), which may limit generalisability; larger multicentric studies would provide more robust statistical validation. Second, the single tertiary-care setting introduces potential referral bias, as such patients may have relatively advanced disease. Third, clinical diagnosis was used as the reference standard and electrophysiological correlation was not uniformly available, so nerve conduction studies could have added functional correlation. Fourth, ultrasonography is operator dependent and inter-observer variability was not formally assessed. Fifth, MRN is limited by cost, availability and longer acquisition times, which may restrict routine use where the leprosy burden is highest. In addition, longitudinal follow-up imaging was not performed, so the role of the two modalities in monitoring treatment response could not be evaluated, and only the ulnar, median and posterior tibial nerves were assessed, excluding other commonly involved nerves such as the common peroneal and radial nerves.

CONCLUSION

Peripheral nerve involvement in Hansen's disease most commonly affects the ulnar and posterior tibial nerves, particularly in patients with multibacillary disease. High-resolution ultrasonography is an effective first-line imaging modality for detecting nerve enlargement, fascicular distortion and tunnel compression, and measurement of nerve cross-sectional area has moderate diagnostic utility, especially for the median and ulnar nerves. MR neurography provides additional information on signal alteration, neuritis, enhancement and deep-nerve involvement, thereby improving overall disease characterisation. Although both modalities detect nerve compression at comparable rates, their agreement is limited, indicating that HRUS and MRN are complementary rather than alternative techniques. The combined use of ultrasonography and MR neurography enhances diagnostic confidence, assessment of disease severity and early detection of complications, thereby facilitating timely management and prevention of permanent disability.

REFERENCES

1. Breen DP, Deeb J, Vaidya S, Lockwood DN, Radunovic A. Leprosy: a common and curable cause

of peripheral neuropathy with skin lesions. J R Coll Physicians Edinb. 2015;45(1):38-42.
2. Trujillo-Ramirez L, Palacios-Ariza MA, Pradilla I, Gamboa LA. Peripheral neuropathy in leprosy: clinical manifestations and disability in a Colombian national referral center. Dermatol Reports. 2021;14(2):9308.
3. Muhaba ES, Geneti SA, Melka D, Mohammed Abdu S. Prevalence, patterns and determinants of peripheral neuropathy among leprosy patients in Northeast Ethiopia: a retrospective study. PLoS Negl Trop Dis. 2025;19(3):e0012944.
4. Venugopal R, Binesh VG, Puthussery PV, George S, Asokan N. Comparison of high resolution ultrasonography with clinical examination in the assessment of peripheral nerve involvement in leprosy. Indian Dermatol Online J. 2021;12(4):536-40.
5. Valls-Solé J. The utility of electrodiagnostic tests for the assessment of medically unexplained weakness and sensory deficit. Clin Neurophysiol Pract. 2016;1:2-8.
6. Martinoli C, Derchi LE, Bertolotto M, Gandolfo N, Bianchi S, Fiallo P, et al. US and MR imaging of peripheral nerves in leprosy. Skeletal Radiol. 2000;29(3):142-50.
7. Dugad K, Pathak S, Rastogi R. Role of high resolution ultrasonography in leprosy. Asian J Med Sci. 2022;13(11):246-53.
8. Tjiaman MP, Zaidan MZ, Ausath ZF, Octaviana F, Karima AP, Menaldi SL. The role of high-resolution ultrasonography (HRUS) in detecting peripheral neuropathy in leprosy patients and household contacts: a systematic review. Lepr Rev. 2025;96(1).
9. Chhabra A, Zhao L, Carrino JA, Trueblood E, Koceski S, Shteriev F, et al. MR neurography: advances. Radiol Res Pract. 2013;2013:809568.
10. Ku V, Cox C, Mikeska A, MacKay B. Magnetic resonance neurography for evaluation of peripheral nerves. J Brachial Plex Peripher Nerve Inj. 2021;16(1):e17-23.
11. Jabeen S, Saini J, Vengalil S, Lavania M, Singh I, Nashi S, et al. Neuroimaging in leprosy: the nerves and beyond. Radiol Infect Dis. 2020;7(1):12-21.
12. Rai T, Singh AM, Indal M, Kumar I. High-resolution ultrasound in evaluation of peripheral neuropathy in patients of Hansen's disease. Indian Dermatol Online J. 2024;15(2):213-7.
13. Bathala L, Krishnam VN, Kumar HK, Neladimmanahally V, Nagaraju U, Kumar HM, et al. Extensive sonographic ulnar nerve enlargement above the medial epicondyle is a characteristic sign in Hansen's neuropathy. PLoS Negl Trop Dis. 2017;11(7):e0005766.
14. Spitz CN, Pitta IJ, Versiani I, Sales AM, Siquara de Sousa AC, Hacker MA, et al. Multimodal approach to the diagnosis of pure neural neuropathy in leprosy. Front Med. 2025;12:1645960.
15. van Brakel WH. Peripheral neuropathy in leprosy and its consequences. Lepr Rev. 2000;71(2):123-39.
16. Voltan G, Filho FB, Leite MN, De Paula NA, Santana JM, Silva CM, et al. Point-of-care ultrasound of peripheral nerves in the diagnosis of Hansen's disease neuropathy. Front Med. 2022;9:985252.
17. Prasangika TG, Senevirathne JK, Sirigampala C, Fernando A, Abeynayake SD, Pandigamage S. Peripheral neuropathy in leprosy among patients attending the dermatology clinic in a tertiary care hospital in Sri Lanka: clinical, ultrasound measures and electrophysiological correlations. Sri Lanka J Dermatol. 2021;22(1).
18. Tagliafico AS. Peripheral nerve imaging: not only cross-sectional area. World J Radiol. 2016;8(8):726-33.
19. Kumar N, Garg RK, Malhotra HS. Ulnar and superficial radial nerve swellings in two patients with leprosy. Am J Trop Med Hyg. 2018;98(4):939-40.
20. Chen Y, Haacke EM, Li J. Peripheral nerve magnetic resonance imaging. F1000Res. 2019;8:F1000 Faculty Rev-1803.
21. Aggarwal A, Das C, Khanna N, Sharma R, Srivastava D, Goyal V, et al. Role of diffusion tensor imaging in the evaluation of ulnar nerve involvement in leprosy. Br J Radiol. 2021;94(1124):20210290.
22. Polavarapu K, Preethish-Kumar V, Vengalil S, Nashi S, Lavania M, Bhattacharya K, et al. Brain and spinal cord lesions in leprosy: a magnetic resonance imaging-based study. Am J Trop Med Hyg. 2019;100(4):921-6.
23. Zhao H, Nepal P, Alam SI. Sonographic evaluation of leprosy of ulnar nerve. Radiol Case Rep. 2021;16(5):1057-60.
24. Upadhyaya V, Choudur HN. Imaging in peripheral neuropathy: ultrasound and MRI. Indian J Musculoskelet Radiol. 2021;3(1):14-23.
25. Reddy Y, Murthy J, Pidaparthi L, Jaiswal S, Kiran E, Penneru A, et al. Sonographic characteristics of median nerve neuropathy in Hansen's disease: a case-control study. Lepr Rev. 2021;92(3):207-17.
26. Lugão HB, Frade MAC, Marques W Jr, Foss NT, Nogueira-Barbosa MH. Ultrasonography of leprosy neuropathy: a longitudinal prospective study. PLoS Negl Trop Dis. 2016;10(11):e0005111.
27. Sharma A, Narang T, Prakash M, Padhi B, Dogra S. Exploring the utility of high-resolution ultrasonography and color Doppler of peripheral nerves in monitoring response to treatment in leprosy patients: a prospective, observational study. Am J Trop Med Hyg. 2024;110(2):1-8.
28. Payne R, Baccon J, Dossett J, Scollard D, Byler D, Patel A, et al. Pure neuritic leprosy presenting as ulnar nerve neuropathy: a case report of electrodiagnostic, radiographic, and histopathological findings. J Neurosurg. 2015;123(5):1238-43.
29. Jain S, Visser LH, Suneetha S. Imaging techniques in leprosy clinics. Clin Dermatol. 2016;34(1):70-8.

30. De Martino Luppi A, Ferreira GE, Borges IS, Antunes DE, Araújo L, Dos Santos DF, et al. Role of multisegmental nerve ultrasound in the diagnosis of leprosy neuropathy. PLoS One. 2024;19(7):e0305808.